Modelling biological and resource fluxes in fluvial meta-ecosystems

Lauren Talluto (talluto@iiasa.ac.at)[1,*], Rubén del Campo (rubendel.campo@um.es)[2], Edurne Estévez (edurne.estevezcano@gmail.com)[3,4], Thomas Fuß (thomas.fuss@uibk.ac.at)[3], Lukas Thuile Bistarelli (Lukas.Thuile-Bistarelli@uibk.ac.at)[3], Jan Martini (jan.martini@uibk.ac.at)[3,5], and Gabriel A. Singer (gabriel.singer@uibk.ac.at)[3]

[1]Biodiversity, Ecology, and Conservation Group, International Institute for Applied Systems Analysis, Laxenburg, Austria
[2]Department of Ecology & Hydrology, University of Murcia
[3]Department of Ecology, University of Innsbruck, Innsbruck, Austria
[4]Faculty of Science and Technology, University of the Basque Country (UPV/EHU), Spain
[5]gutwasser GmbH, Geerenweg 2, 8048, Zürich, Switzerland
[*]Author for correspondence.

Paper type:
Short title: Modelling fluvial meta-ecosystems
Keywords: fluvial meta-ecosystems, biodiversity, ecosystem functioning, nutrients, river networks

Abstract

Meta-ecosystem theory predicts that cross-ecosystem flows of energy, nutrients, and organisms have important implications for local community assembly and ecosystem functioning. Developments in the theory also have the potential to enhance our understanding of biodiversity-ecosystem functioning relationships. Meta-ecosystem theory is particularly well-suited to the study of rivers, because water flow forces strong spatial interrelationships among connected ecosystems. However, models that address flows of both resources and organisms and explicitly link both are lacking. We present a model and associated R-package for cross-ecosystem flows of both resources and organisms that can be used to predict their distribution in river networks, as well as meta-ecosystem functioning. The model incorporates feedbacks between these two crucial components—resource concentrations represent niche dimensions for organisms, modifying the colonisation and extinction dynamics and different locations in the network, and organisms also consume resources, thereby modifying the concentrations that are transported downstream. To illustrate the capabilities of the model, we present an in silico experiment and analysis, as well as providing sample code.

1 Introduction

Understanding the effects of biodiversity on ecosystem functioning (EF) has long been a central goal of ecological research (Bannar-Martin et al. 2018). In general, biodiversity is an important driver of EF (Cardinale et al. 2012; Hooper et al. 2012) and can be as important as abiotic drivers (e.g., climate Duffy et al. 2017), leading many researchers to hypothesise that ecosystems with more species would exhibit higher levels of EF (Margalef 1963). However, recent experiments and models have revealed complex effects of diversity on EF (i.e., positive, negative and no effects; see Pennekamp et al. 2018), pointing to non-linear and context dependent biodiversity-EF relationships (Thébault and Loreau 2006; Little and Altermatt 2018). This further suggests additional important drivers of EF beyond the diversity of organisms. For example, the rates of acquisition, use and allocation of resources are key EFs that can depend on species composition (and corresponding functional traits) due to the effects of morphology, behaviour, and physiology (Hooper et al. 2005; Díaz et al. 2013; Gagic et al. 2015). Moreover, different resources contain different essential nutrients and carbon compounds that determine lability and palatability; thus resource properties can also strongly determine consumption and processing rates (Cornwell et al. 2008).

River networks are characterised by high biodiversity, variability in spatial structure, and large fluxes of energy, nutrients, and organisms among ecosystems. This is in large part due to the overwhelming imprint that the flow of water has on the spatial structure of fluvial networks. In particular, the relative isolation of less-connected upstream portions of a fluvial network contrasts strongly with downstream areas where water flow brings organisms and nutrients from many upstream regions. Moreover, because water flow is temporally variable, the degree of connectivity is similarly dynamic. Finally, rivers are embedded in a terrestrial environment, implying that the physical and geographical structure of river networks promotes the exchange of resources and organisms both between aquatic and the surrounding terrestrial ecosystems, as well as among different locations in the river (Cid et al. 2022; Battin et al. 2008). These processes have profound implications for community assembly and EF. The spatial structure of a river network, and the degree to which this structure differentially influences the movement of organisms and materials, may significantly impact EF at the scale of the entire network (Talluto et al. 2024). Recent developments in the theory of meta-ecosystems provide a solid conceptual framework for describing how both organisms and material interact in such a spatial context, and how this interaction can influence the spatial distribution of EF (Loreau et al. 2003; Gravel et al. 2010; Harvey et al. 2023).

Despite developments in theory, field studies of meta-ecosystems are challenging due to the complexities of the processes, the disconenct between theoretical processes and what is feasible to measure in the field, and the multiple spatial scales generally involved in most meta-ecosystems (Gounand et al. 2018). In order to better integrate the theory of meta-ecosystems with actual field studies, we need both (i) highly resolved spatio-temporal data on resources and organisms within fluvial meta-ecosystems (FMEs), and (ii) a new generation of models operating at the meta-ecosystem level (Talluto et al. 2024). These models should link community composition with resources and EF. The availability of datasets is rapidly increasing thanks to technological developments that allow for greatly improved resolution in studying both community

composition (e.g., through eDNA and metabarcoding) as well as resource composition diversity (e.g., size-exclusion chromatography, mass spectrometry and infrared spectroscopy) (Sleighter and Hatcher 2008; Huber et al. 2011; Tremblay et al. 2011; Baird and Hajibabaei 2012). These datasets are unprecedented in both breadth—covering a great spatial extent, such as entire river networks—and depth—capturing much more biological and chemical diversity at a single location than has ever been possible (Altermatt et al. 2020). However, we still lack models that can provide the context for these datasets at the appropriate spatio-temporal scales (Gounand et al. 2018; but see Harvey et al. 2023).

Developing fluvial meta-ecosystem models presents important challenges due to the unique properties and structure of river networks. For example, the spatial configuration of river networks imposes unique and strong controls on both organisms and resource fluxes. However, the distribution of these ecosystem components is driven by different mechanisms. Resources highly depend on structure of the surrounding terrestrial ecosystem (i.e., land cover shapes the nature of the resources that are transferred to the river corridor) and are passively transported by flow (Roebuck et al. 2020). In contrast, the distribution of organisms is driven by the interplay between (i) stochastic processes (e.g., extinctions); (ii) dispersal (including both flow-mediated downstream dispersal but also active dispersal and transport by other organisms); (iii) local environmental factors, including resource properties, that filter species from the regional species pool; and (iv) biotic interactions (Leibold et al. 2004; Urban 2004; Heino et al. 2015).

Here, we develop a meta-ecosystem model that explicitly couples the distribution and fluxes of both resources and organisms in FMEs. We construct this model by joining two commonly-used model types in fluvial ecosystem and community ecology: transport-reaction models (for resources), and metacommunity models (for organisms). By linking these two models, we allow for feedbacks between the organisms and the resources they use. These feedbacks are essential to enable a more mechanistic understanding of the connections between the processes underlying community assembly, resulting biodiversity patterns, and EF. Our model structure facilitates developing and testing *in-silico* hypotheses regarding FME properties. These properties can include, for example, interactions of biological communities with resources in the context of river spatial structure, and bothlocal- and regional-scales, and the consequences of these interations on patterns in biodiversity and EF, The model also allows for manipulations of river connectivity, flow, resource and organism traits, and the terrestrial matrix. We provide an implementation of the model via an R-package as well as some worked examples with sample code and data.

2 Materials & Methods

2.1 Model Description

Our conceptual starting point for modelling the biological community is metapopulation theory (Levins 1969). The classic metapopulation model tracks the number of occupied patches p in a landscape composed of h available patches as a function of the rates of colonisation and extinction of local populations within those patches:

$$\frac{\partial p}{\partial t} = cp\,(h - p) - pm \tag{1}$$

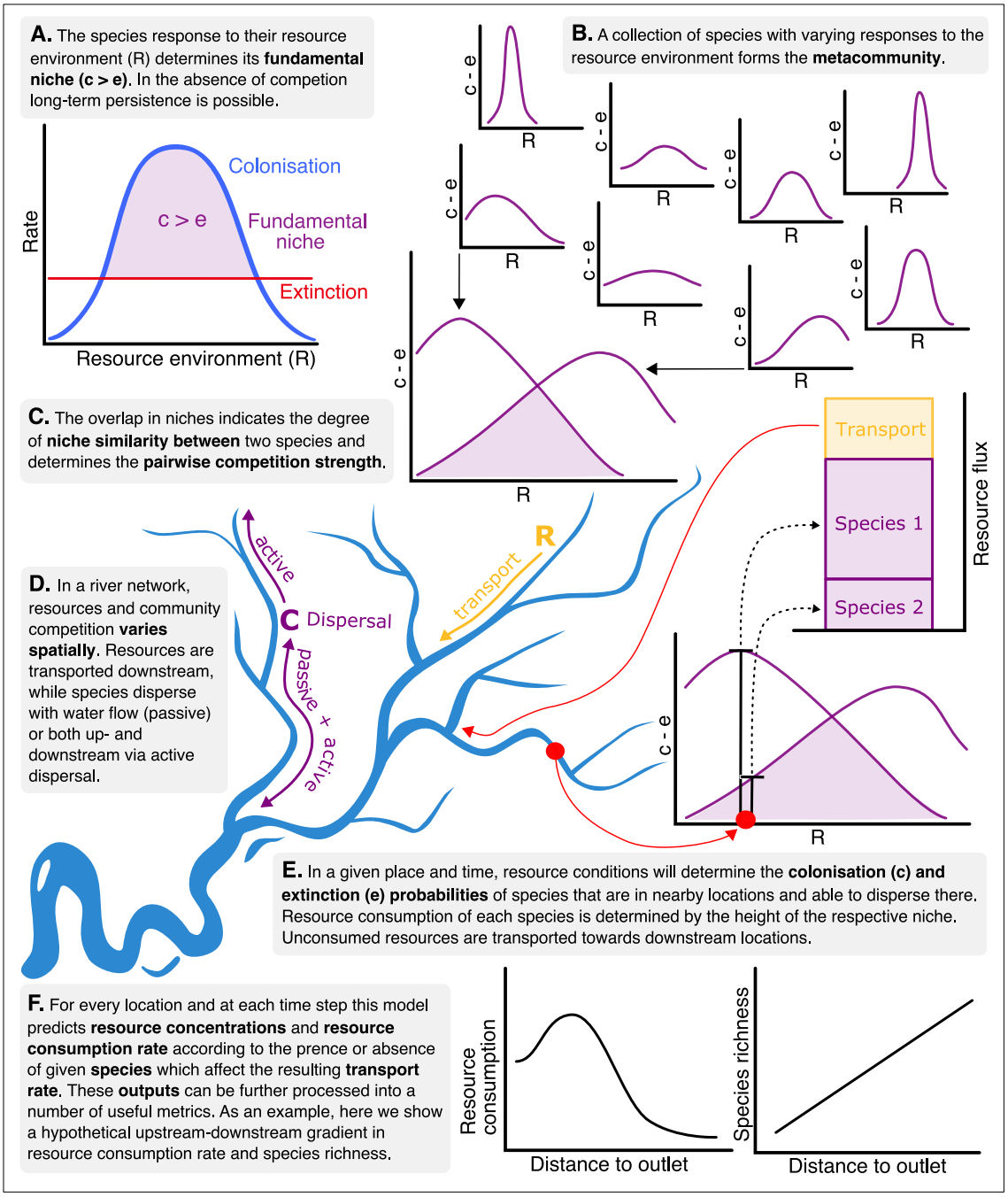

Figure 1: Conceptual diagram illustrating key model flows and outputs.

In this model, extinction occurs within occupied patches according to the extinction rate m, resulting in the total negative occupancy flux of pm. Similarly, unoccupied patches are colonised according to the colonisation rate c. The additional p in the colonisation term takes dispersal into account; as more patches are occupied in the metapopulation, unoccupied patches are colonised more quickly due to increased dispersal from the occupied patches.

Hunt and Bonsall (2009) extended this model to multi-species communities by adding competition to the extinction term:

$$\frac{\partial p_i}{\partial t} = c_i p_i \left(h - p_i\right) - p_i \left(m_i + \sum_{j \in \mathbb{S} \setminus \{i\}} m_{ij} p_j\right) \tag{2}$$

where the subscript i indicates a focal species, the subscript j a competitor, and $\mathbb{S} \setminus \{i\}$ is the set of species in the metacommunity excluding the focal species i. Here, the extinction rate is now broken into two terms. The first a species-specific intrinsic extinction rate m_i, representing, e.g., stochastic extinctions that are unrelated to other species. The m_{ij} term is the effect of competition between i and j on the extinction rate of i (multiplied by p_j because competition only occurs when species j is also present). For future clarity of notation, we assume all parameters are specific to a target species i and thus omit the subscript.

The model in equation 2 describes regional dynamics; the rates of dispersal, competition, colonisation and extinction are constant across all locations in the metacommunity. However, these rates certainly vary in space in real metacommunities, particularly in rivers where habitat conditions and river flow follow strong gradients (e.g., discharge generally grows moving from upstream to downstream). We first consider how river flow interacts with dispersal in local communities (denoted by the subscript k). In rivers, hydrological connections among habitat patches facilitate passive dispersal with flowing water. In addition, many organisms are capable of active dispersal (i.e., any dispersal not facilitated by the flow of water in the river channel), either overland or upstream along the river course, and even organisms that cannot move themselves can be carried upstream by various processes (e.g., transport by other organisms, wind, or humans; Kristiansen 1996). Because these two dispersal modes are likely to occur at quite different rates, and because the rates will likely vary among different types of organisms, we break the dispersal portion of the colonisation term here into active (α) and passive (β) components, with the passive component additionally weighted by the input discharge Q_k. Finally, local dispersal is weighted by the occupancy of reaches within dispersal range (denoted with k').

$$\frac{\partial p_k}{\partial t} = \begin{cases} c\left(\sum p_{k'}\alpha + \sum p_u Q_u \beta\right) & p_k = 0 \\ m + \sum_{j \in \mathbb{S} \setminus \{i\}} m_j p_j & p_k = 1 \end{cases} \tag{3}$$

It should also be noted that, since this equation is local, only one of the colonisation or extinction flux will apply at any given time, depending on whether the site is occupied.

An additional important factor is variation in the local environment, which could contribute both to colonisation and extinction fluxes. The Levins model (eqn. 1) has been extended by more recent theoretical (Holt and Keitt 2000; Holt et al. 2005) and empirical (Talluto et al. 2017) work by fitting the colonisation and extinction rates as functions of local climatic conditions.

The result is a dynamic range model with long-term occupancy driven by the balance of local colonisation and extinction (Talluto et al. 2017). We combine this approach with the multi-species Hunt model (eqn. 2) by redefining the c and m terms to be functions of the quality q_k of the focal patch:

$$\frac{\partial p_k}{\partial t} = \begin{cases} c\left(q_k\right)\left[\sum p_{k'}\alpha + \sum p_u Q_u \beta\right] & p_k = 0 \\ m(q_k) + \sum_{j \in \mathbb{S} \setminus \{i\}} m_j p_j & p_k = 1 \end{cases} \tag{4}$$

The shape of these two functions is flexible; for example, Talluto et al. (2017) defined them as quadratic functions of local climate conditions. Our more general approach here can incorporate local climatic and/or habitat conditions, and dynamic resource concentrations into the q term. We explore these possibilities further in the case studies. For now, we consider the case where $q_k = [R]_k$, the concentration of an essential resource. We can use a simple transport-reaction model (Soetaert and Herman 2009) to describe the fluctuations of this resource concentration in time and space (since all terms relate to a focal patch, the subscript k has been omitted for clarity).

$$\frac{\partial R}{\partial t} = \sum_{i \in S} R\rho_i(R) - \frac{QR - \sum Q_u R_u}{Al} \tag{5}$$

The first term on the right hand side models reaction; we consider here only reaction due to biological activity, and postulate that the net reaction in a patch is the sum of a set of resource use functions, $\rho_i(R)$, of all species $\mathbb{S}$ in the local community. Each ρ_i function describes the impact of a species on the resource in units of s^{-1}. The forms of these functions will depend on which resources are being modelled. The second term gives loss due to advective transport, where Q is the discharge of the focal patch (in volumetric units per unit time; we use $\mathrm{m}^3\ \mathrm{s}^{-1}$ throughout). Each patch receives inputs both in the form of lateral flow (e.g., overland flow, groundwater, etc.) as well as flow from upstream reaches. Thus, the total input resource mass for the focal patch will be the sum of input masses, which are the product of the input concentrations (R_u) and discharges (Q_u). Finally, the masses are converted back to a concentration using the cross-sectional area (A; m^2), and length (l, m).

2.2 Implementation

We provide an implementation of the model in an R-package **flume** (FLUvial Meta-Ecosystem model) (Talluto 2023), and demonstrate some capabilities via case studies and sample code. In this section we describe some of the implementation details that are flexible in the formulation of the model above, but for which we have made specific choices in software. A full list of model parameters and default values from the package is available in Table 1.

2.2.1 Patch quality

Patch quality is defined by two functions describing the impact of quality on colonisation and extinction (eqn. 4). We modelled the colonisation niche (i.e., the shape of the c function) as a Gaussian curve (Austin 1999). Thus, for a single resource, the niche shape can be defined by

Table 1: Model parameters with defaults and values used for case studies.

Symbol	Description	Default Value	Case Study 1	Case Study 2
c_μ	Niche location	$0 - 1^*$	$0.1 - 0.9$	varies ‡
c_σ	Niche breadth	$c_{\mu,2} - c_{\mu,1}$ †	0.1	varies ‡
c_γ	Colonisation scale	5×10^{-6}	6×10^{-6}	varies ‡
m_γ	Extinction scale	2×10^{-7}	1.25×10^{-7}	varies ‡
α	Active dispersal rate	0.1	$0.05 - 2.8$	0.5
β	Passive dispersal rate	0.1	0.1	0.1
o_γ	Competition scale	0.001	$0.001, 0.1$	1×10^{-4}
r	Resource use scale	5×10^{-4}	5×10^{-4}	1×10^{-3} N, 5×10^{-4} P

*Uniformly distributed across the range, depending on the number of species.

† i.e., the distance between niche locations of adjacent species.

‡ Parameters determined empirically, see §3.2

three parameters: location (c_μ), breadth (c_σ), and scale (c_τ):

$$c(R) = c_\tau e^{\frac{-(R-c_\mu)^2}{2c_\sigma^2}} \tag{6}$$

With multiple niche dimensions, the niche shape is similarly described by a multivariate Gaussian. Extinctions in the model can be constant with respect to the environment, controlled only by a scale parameter (m_γ), or can follow an inverse Gaussian with a location, breadth, and scale.

2.2.2 Competition

Our metacommunity model includes a competition term ($\sum m_i j p_j$), allowing for totally independent pairwise (and potentially asymmetrical) competition coefficients among species. In practice, pairwise competition strength is extremely difficult to estimate. Thus, we make a simplifying assumption that the strength of competition will be proportional to the degree of overlap in two species' fundamental niches (defined as the difference between colonisation and extinction, excluding the competition term). We further add a scale parameter o_γ (which is constant by default but can vary by species pair). In flume, we compute this as the area of overlap in the two species' niches, represented mathematically as the integral of a piecewise function defined by the lesser of the two species' niches when both niches are positive (i.e., within the fundamental niche of the species), and zero otherwise:

$$m_{ij} = o_{\gamma,ij} \int \begin{cases} c_i(R) - m_i(R) & 0 < c_i(R) - m_i(R) \leq c_j(R) - m_j(R) \\ c_j(R) - m_j(R) & 0 < c_j(R) - m_j(R) < c_i(R) - m_i(R) \\ 0 & 0 \geq c_j(R) - m_j(R) \\ 0 & 0 \geq c_i(R) - m_i(R) \end{cases}$$

2.2.3 Resource use functions

In principle, we expect that a species' total resource consumption at a patch will be correlated with its abundance (or biomass) (Díaz et al. 2003; Winfree et al. 2015). Although we do not track abundance in our model, we can make the simplifying assumption that abundances will

be higher when species are closer to their niche optima (Holt et al. 1997; but see McGill 2012). Thus, the consumption $\rho_i(R_k)$ by species i at site k (eqn 5) will be proportional to the niche height at that site $c_{i,k} - m_{i,k}$ (eqn. 4). We can further allow that species vary in their ability to use resources, scaling the resource use function by a species-specific consumption constant r_i:

$$\rho_i(R_k) = \begin{cases} r_i \frac{c_{i,k} - m_{i,k}}{\max(c_i - m_i)} & c > m \\ 0 & c \leq m \end{cases} \tag{7}$$

Here we scale the niche height by the maximum niche height to allow us to interpret this term as the fraction of a species' maximum consumption rate, and to interpret r_i as the maximum rate. Finally, we assume that when a species is outside its equilibrium habitat (i.e., when $m > c$; Talluto et al. 2017), resource consumption is negligible and can be ignored.

2.2.4 Stochastic simulations

For analysis, we discretised the model in space and time. We thus consider a series of habitat patches representing stream reaches. Each reach is characterised by two fundamental state variables: the resource vector $\mathbf{R}$, giving the concentration of each resource, and the community vector $\mathbf{C}$, which gives the absence (denoted by zeroes) or presence (denoted by ones) of all possible species in the community. For any time interval Δt we can then compute the probability of observing colonisations and extinctions for a species i (eqn. **??**):

$$\begin{aligned} \mathrm{pr}\left(\mathbf{C}_{i,t+\Delta t} = 1 \mid \mathbf{C}_{i,t} = 0\right) &= 1 - \mathrm{e}^{-c_i p_i (\alpha_i + \beta_i Q)\Delta t} \\ \mathrm{pr}\left(\mathbf{C}_{i,t+\Delta t} = 0 \mid \mathbf{C}_{i,t} = 1\right) &= 1 - \mathrm{e}^{-(\sum m_{ij}\mathbf{C}_{j,t} + m_i)\Delta t} \end{aligned} \tag{8}$$

Here, the prevalence term p_i indicates local prevalence, i.e., the number of occupied reaches within dispersal range. We consider only the case of nearest neighbour dispersal, so p_i is the sum of the occupancy states of reaches immediately up- and downstream of the focal reach; longer distance dispersal can be incorporated via the regional species pool (see §**??**).

Changing resource concentration can be computed for each reach using a variety of numerical integration techniques. The flume package uses the lsoda algorithm implemented in the DeSolve R-package (Soetaert et al. 2010).

2.3 Boundary Conditions

Boundary conditions in the model are used to represent external input into the river network (e.g., input of resources and organisms from the terrestrial environment, or overland flow of water and groundwater contributing to discharge). Rivers are not closed systems, and because of the downstream flow of water, all material would be rapidly flushed downstream without user-provided boundary conditions. In the model, these inputs are provided by a virtual reach with a constant user-defined resource composition and community composition. Thus, model terms that incorporate water flow from upstream (e.g., resource transport and passive dispersal) will incorporate inputs both from upstream in the river as well as from outside the river network. Lateral discharge from these reaches is not user supplied, rather it is computed as the growth in

discharge from one reach to the next moving downstream, according to the growth in catchment area and defined by hydraulic scaling relationships (Burgers et al. 2014). By default, flume uses boundary conditions as initial conditions as well, but this can be overridden. The actual resource concentration and community composition of the virtual reaches can vary depending on modelling needs; for example, community composition could be uniform and contain all possible species to represent a classical "regional species pool" from metacommunity modelling, or resource concentrations could vary among headwaters or from upstream to downstream to represent land use gradients.

2.4 Temporal resolution

The time scale of the model determines how frequently colonisation and extinction steps are performed; community state is constant within time steps. The temporal resolution is set via a parameter passed at model initialisation, with units determined by the units of discharge. The default value is 86400, which, assuming discharge is in units of m^3s^{-1}, corresponds to 24 hours. Thus, using default parameters, community composition can change once per day, while resources are integrated continuously throughout the day. Longer time steps can be set to simulate slower community dynamics and improve computation time, with the potential downside that this allows resource concentrations to change more while community composition is constant.

2.5 Model output

After a simulation run, the model returns an object containing all model parameters and complete state (i.e., the model is resumable). The object also contains a complete history of all state variables, consisting of reach by time by resource and reach by time by species arrays. Resource fluxes (transport and consumption) are also returned for every reach and time step and are the primary metrics of EF returned by the model. The package also includes a variety of convenience functions for plotting and for computing aggregate metrics for both community and resource state.

2.6 Sample river network

In order to demonstrate some features of the package and explore the behaviour of the model, we created a representation of the Kamp river in Austria to use as the spatial setting for simulations. This river network is included with the package, along with other sample networks, and a vignette is included to help users generate a network from a digital elevation model.

3 Case studies

3.1 Case Study 1: Effects of dispersal and competition on biodiversity-EF relationships

For local communities, we expect that a strong match between environmental/resource conditions and the niches of occurring species should result in efficient use of resources and thus high

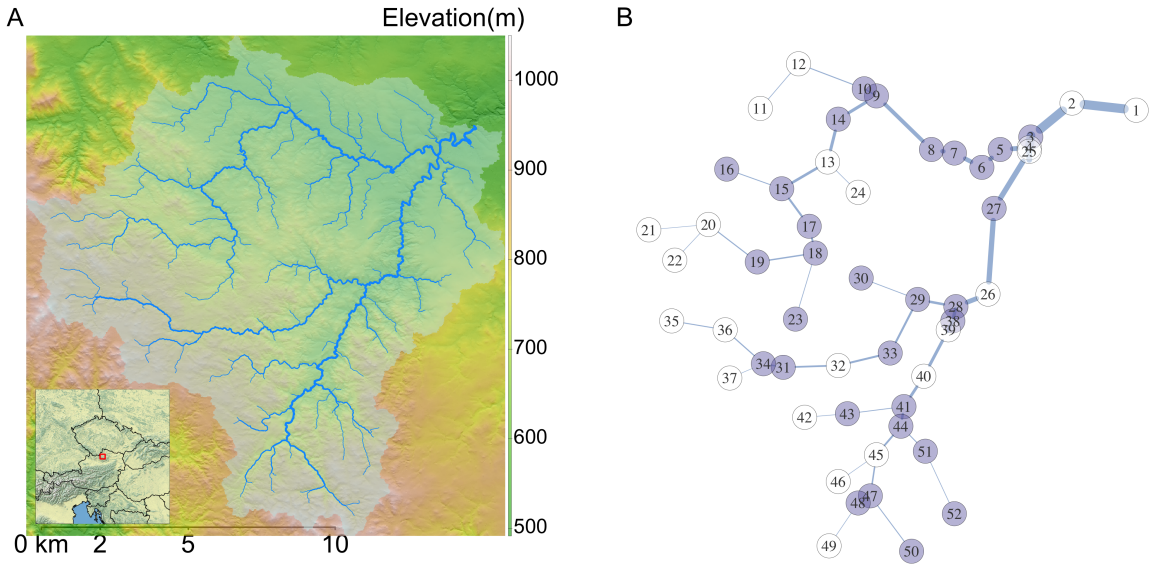

Figure 2: (A) Delineated Kamp river network, with the drainage area shown shaded. Line weights are proportional to Strahler stream order. Location of the river network within central Europe is shown in the inset. (B) Schematic of the Kamp river network after conversion for use with flume. Line weights are proportional to discharge, which ranges from 0.05–0.88 $m^3 s^{-1}$. The network has been segmented into approximately 2-km reaches (which are assumed to be exactly equal length for modelling purposes); each node in the schematic is a reach midpoint. Reaches containing sampling sites (used in Case Study 2) are highlighted in purple.

local EF. It follows that, in order to achieve such a strong match, species that have appropriate niches must both exist and have the ability to reach local sites with the right conditions. A large regional species pool (i.e., high γ diversity) makes it more likely that species with fitting niches are available; thus at the network scale we expect γ diversity to correlate with the strength of biodiversity-EF relationships (i.e., networks with high γ diversity will have, on average, local communities with stronger biodiversity-EF relationships). However, γ diversity can only increase functioning if species are able to get to appropriate habitats. Thus, dispersal may be an essential mediator of biodiversity-EF relationships. If species are dispersal limited, then many niches may be vacant, resulting in local communities that cannot efficiently process resources and thus have low EF. On the other hand, high dispersal can lead to communities structured primarily by mass effects, resulting in communities with many redundant species or with species that are not well-adapted to local conditions (Mouquet and Loreau 2003; Declerck et al. 2013; Horváth et al. 2016). In other words, dispersal being either too low or too high can lead to a mismatch between environment and species and may reduce the strength of biodiversity-EF relationships.

We developed scenarios to see whether flume can reproduce the expectation that local-scale biodiversity-EF relationships are stronger at intermediate dispersal. We included γ diversity and the strength of competition as additional variables, to determine if they mediate any effect of dispersal on biodiversity-EF relationships. Using the Kamp river network (Fig. 2) as the spatial template, we started with a template metacommunity consisting of 50 species. All species had identical niche parameters (Table 1), with the exception of the niche location, which was

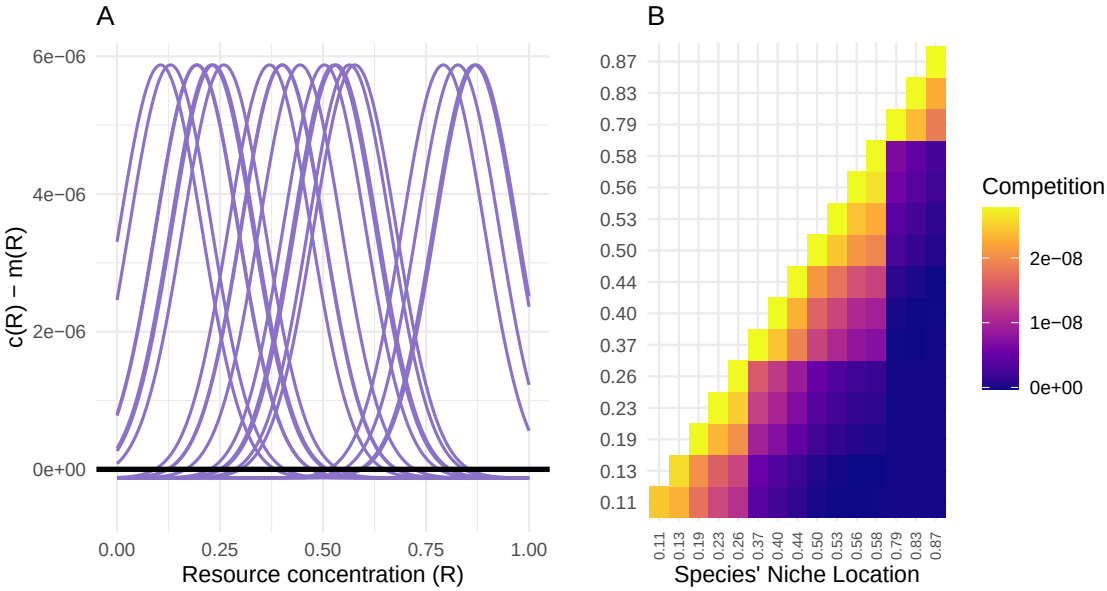

Figure 3: Visualisation of (A) niches and (B) strength of competition for a sample metacommunity of 20 species. In (A), the vertical axis is the difference between the colonisation term $c(R)$ and the extinction term $m(R)$. The height of this curve represents the net rate of change of occupied patches for given resource conditions for each species. Values greater than zero indicate conditions under which the species is able to persist in the long-term and represent the species' fundamental niches. In (B), species are ordered following their niche location (i.e., the location on the resource axis of the optimum in A). Colours indicate pairwise competition strength, which are proportional to the degree of niche overlap.

randomly selected on the interval (0.1, 0.9). We scaled resource concentrations such that they were approximately between 0 and 1, for simplicity. From this template, we generated scenarios consisting of either a high- (40 species) or low- (20 species) diversity metacommunity. These scenarios were generated by drawing species randomly from the template metacommunity; for each diversity scenario, we generated a total of ten metacommunities this way, each with different randomly drawn species (Fig. 3).

For each of the ten randomly generated metacommunities, we ran simulations while varying dispersal ability and the strength of competition. Competition strength was varied by adjusting the competition scale parameter. In this way, local competition was always dependent on the number and niche parameters of species present, but globally competition was scaled up or down according to the scenario. We ran a high-competition scenario ($o_\gamma = 0.1$) and a low-competition scenario ($o_\gamma = 0.001$). We varied dispersal by changing the active dispersal component (α) from $\alpha = 0.4$ to $\alpha = 2.8$, in steps of 0.4. We additionally added a "nearly zero" dispersal scenario where $\alpha = 0.05$, for a total of eight dispersal scenarios. We used a small value instead of zero for α to avoid species being permanently lost from upstream reaches due to no upstream dispersal (and no immigration from outside the river network). The passive dispersal parameter was held at a constant low level ($\beta = 0.1$). All combinations of competition, γ-diversity, species lists, and dispersal ability resulted in 320 total scenarios. Additionally, to capture variability in the stochastic model, we replicated each individual scenario 8 times. All scenarios were run at a temporal resolution of 1 day, and for a total of 90 time steps. Boundary conditions for resources

were set to vary between 0.1 and 0.9 and were set to simulate a resource gradient due to, e.g., land use differences across the river network (Fig XX). Initial resource concentrations were set to match the concentration of input from the boundary conditions; we found in initial testing that, in the absence of fluctuations due to community changes, initial conditions had very little impact on model state since the river network quickly reaches an equilibrium resource state. Initial species locations were determined randomly with a per-species target prevalence of 20% of reaches occupied. For reporting results, we use a temporal average from the final 30 time steps. Taking the last time steps allows the model time to "forget" initial conditions, while averaging over time reduces some noise simply due to random fluctuations in colonisation/extinction of species. We use the total resource consumption rate (i.e., in units of $mass \times volume^{-1} \times time^{-1}$) as the measure of EF, and species richness as the measure of biodiversity.

The extent to which dispersal reduced the efficiency of resource processing depended both on γ diversity and competition strength. The strength of the biodiversity-EF relationship also depended both on γ diversity and competition strength. When competition was weak, we observed little relationship between the biodiversity-EF slope and the dispersal ability of species when diversity was low, but a weak negative relationship when diversity was high (Fig. 4). For both of these scenarios, there was no hump shape; i.e., the theoretical prediction that dispersal facilitates strong biodiversity-EF relationships up until mass effects result in poorly adapted communities was not supported when competition was weak. In contrast, with strong competition, we observed a pronounced hump in the relationship between the biodiversity-EF slope and dispersal ability. In high diversity-high competition scenarios, the decline in the biodiversity-EF slope was quite rapid following its maximum, suggesting that with many available species, mass effects quickly overwhelm local sorting (Fig. 4b). For low diversity-high competition scenarios, this decline was more gradual.

3.2 Case study 2: Periphyton community structure in response to changing N:P ratios

For a second case study, we integrate field measurements with an *in silico* experiment to explore how point-source nitrogen pollution could influence biodiversity of periphyton in a network, while using a topology derived from a real river. We use dissolved inorganic nitrogen (DIN, in mg/L) and soluble reactive phosphorous (SRP, mg/L) measured at 32 sites in the Kamp river (Fig. 2). We set the model to separately track N and P concentrations; however, when determining the niche of species, we used the N:P ratio. This ratio can be an important determinant of periphyton community structure in rivers (Stelzer and Lamberti 2001). Moreover, this use highlights the capability of the model to use metrics derived from multiple resources as a single niche dimension.

At the same sites, periphyton community composition was measured by metabarcoding. We scraped off biofilm from the sun-facing side of at least 10 randomly collected stones per site and extracted DNA via DNeasy PowerSoil Pro Kit (Qiagen, Germany). LGC Genomics Gmbh (Berlin, Germany) performed the amplification of the 18S rRNA using primers DIV4for: 5'-GCGGTAATTCCAGCTCCAATAG-3' and DIV4rev3: 5'-CTCTGACAATGGAATACGAATA-3' (Visco et al. 2015; Zimmermann et al. 2011; Zimmermann et al. 2015), library preparation

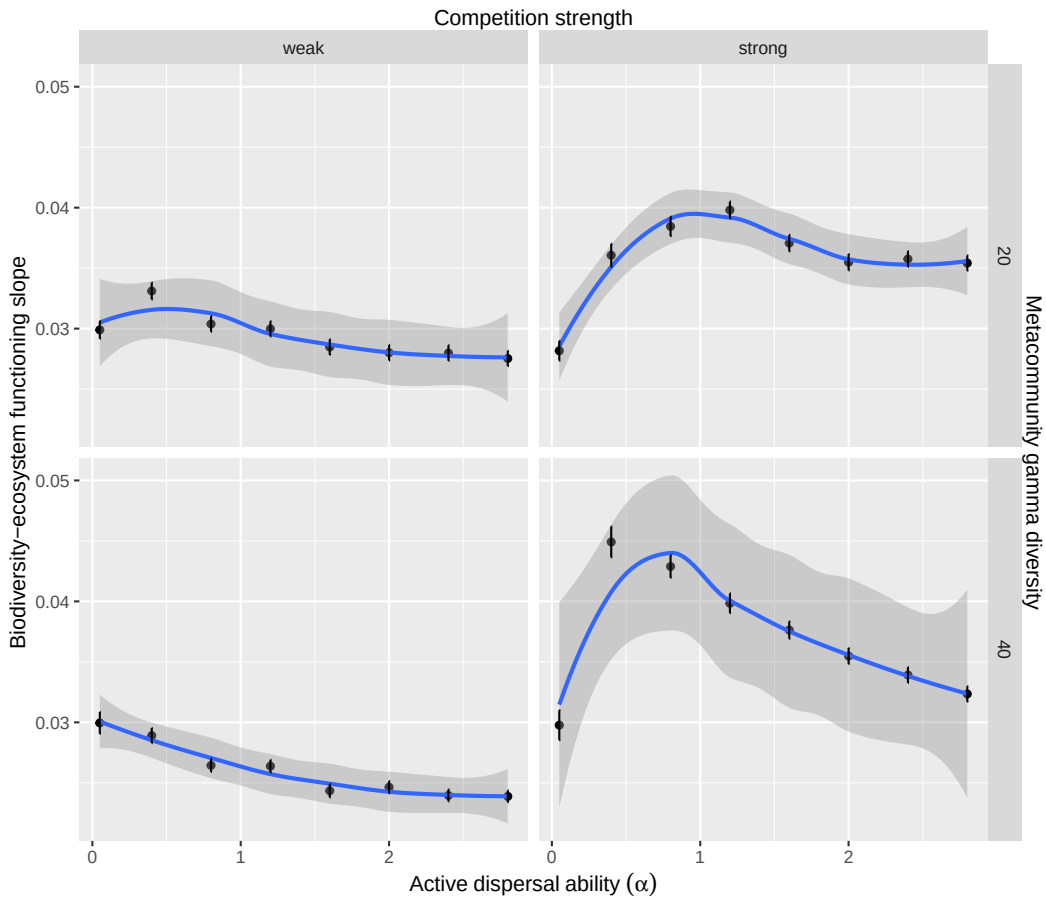

Figure 4: Strength of the biodiversity-EF relationship as a function of dispersal. Columns show weak (left) and strong (right) competition scenarios, while rows show low (top) and high (bottom) metacommunity diversity scenarios. A loess smoother has been added to show the relationships more clearly. When competition is weak, there is little relationship between dispersal and biodiversity-EF relationships. In contrast, strong competition facilitates a strong link between biodiversity and EF, with maximum slopes observed at low to intermediate dispersal rates.

(2 x 300 bp) and sequencing on a MiSeq Illumina platform. Finally, species were obtained as amplicon sequence variants (ASVs) using the DADA2 R package (Callahan et al. 2016; Callahan et al. 2017). (for complete sampling methods, periphyton sampling methods and water chemistry methods follow (Fuß et al. 2024b) and DNA extraction follows (Fuß et al. 2024a)). From the complete community dataset, we retained the 40 most abundant ASVs that were present at at least ten reaches. For modelling, niche optima and breadths were computed as the abundance-weighted mean and sd of the N:P ratio for each taxon.

To establish initial conditions for resources in the network, we used measured values if available, and performed discharge-weighted linear interpolation for all other reaches. Boundary conditions for resources (i.e., the concentrations of resources from lateral input) were identical to the starting conditions. We also assumed that algae dispersed from outside the river network (e.g., via overland flow, animal-mediated dispersal, wind, etc). We computed out-of-network dispersal rates proportionally to the downstream growth in catchment area; upstream nodes with small catchments had relatively low outside dispersal flux, while a reach that is much

larger than

We conducted this experiment in a similar manner as in case study one, setting up simulations for scenarios (replicated twenty times each) resulting from the variation of three parameters. First, we varied location to see if the topology of the scenario had any impact on how point source pollution affected diversity throughout the network. For pollution sources, we used one reach very near the headwaters (reach 34), and two reaches at intermediate distances from the headwaters but in different subcatchments (reaches 15 and 41; see Fig. 2). Second, we varied the input concentration of N, with levels of 15, 30, and 60 mg/L, equivalent to roughly 0.5–2 times the maximum concentrations for wastewater discharge in the European Union (Fernández-Nava et al. 2008; Directive 91/271/EEC 1991).

Finally, we varied the input discharge of the pollution source with levels of 50, 100, and 200 L/second.

We ran the model at a daily time scale allowing for 100 days of equilibration at initial conditions. We then applied the pollution treatment and ran the model for an additional 130 days at the new conditions, the first 100 of which were discarded to allow the system to equilibrate. We report results as averages across all twenty replicates and across the final 30 days of simulation.

All pollution treatments had a strong negative effect on asv richness at the source, and in most cases these effects persisted downstream, although the strength of the effect decreased with distance from the source (Figs. 5, 6, 7). We also observed a slight decrease in richness upstream from the source, suggesting that, with these parameters, continuity of habitat is important for facilitating upstream dispersal (Fig. 7, middle panel). Interestingly, at lower levels of pollution, reach 4, which is a confluence where the two major subcatchments meet, became a diversity hotspot. (Fig. 7, middle and bottom panels). In this case, the non-polluted tributary acts as a diversity refuge for taxa intolerant of pollution, and the dilution provided by the "clean" tributary reduces the N:P ratio to a point where many taxa can coexist. Thus, the combination of a diverse pool of dispersing organisms and favourable chemical conditions results in a much more diverse community than what is observed in the control.

To examine how pollution affected periphyton community composition, we computed Jaccard dissimilarity using a presence-absence matrix. We considered a taxon to be locally present if it occurred in a reach in at least 8 of the last 30 days of the simulation. We took the median Jaccard value by reach pair across replicate simulations for each scenario. We then computed a principal coordinates analysis (PCoA) on this matrix, and plotted first two axes as an index of periphyton community composition. When pollution concentrations were high, the index of community composition showed large changes throughout the network, however these changes are likely due to the collapse in asv richness in these scenarios (Fig. 7). At lower pollution loads, we observed changes in community composition in some cases, depending on the origin point of the pollution. Interestingly, even nodes that were not hydrologically connected to polluted reaches experienced changes in community composition, possibly showing that the disruption to connectivity/dispersal influences community structure broadly across the network (Fig. 8).

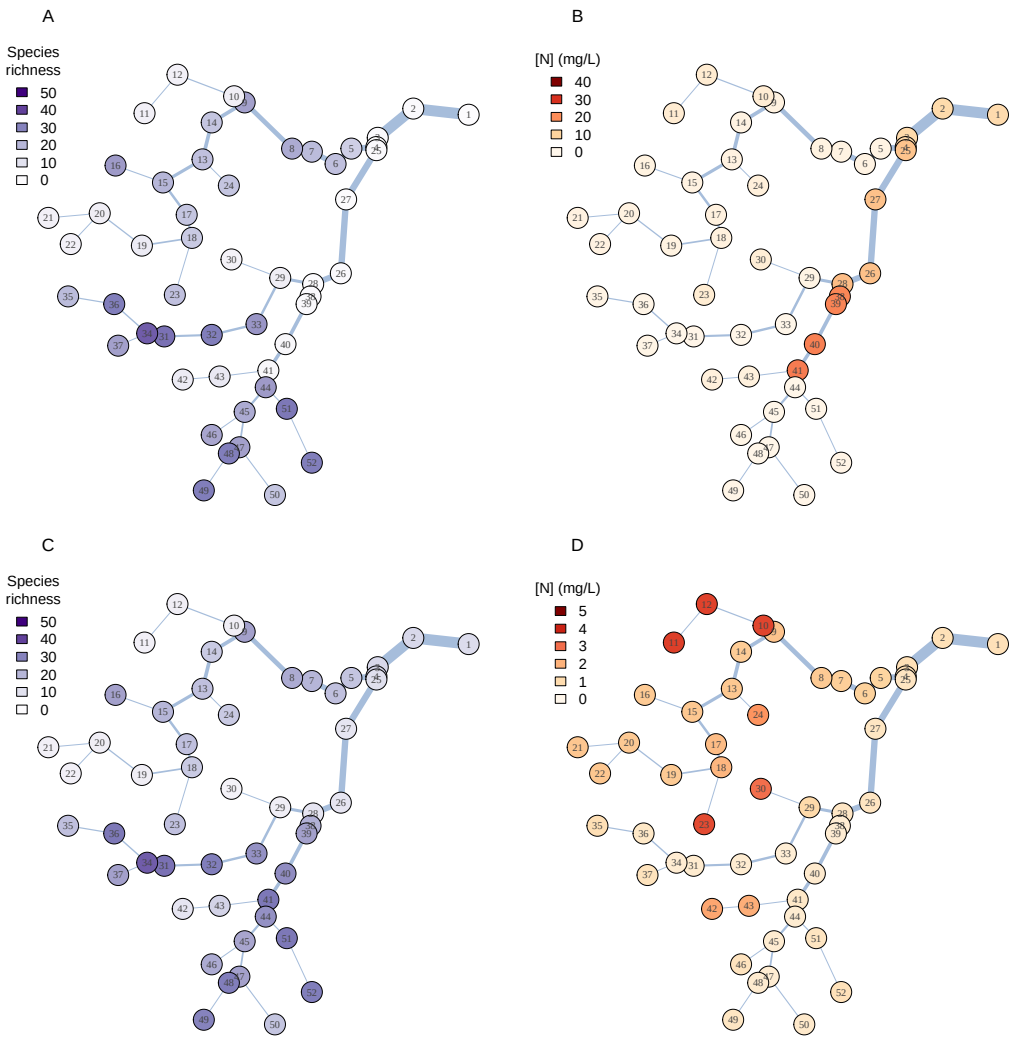

Figure 5: Comparison of periphyton asv richness (A, C) and pollution concentrations (B, D) for the strongest pollution treatment (A, B; N source concentration = 60 mg/L, Q = 200 L/s) and control (C, D). Pollution effects and associated declines in richness persist along the entire length of the stream from the source (reach 41). Note the different scales for nitrogen concentration in B and D.

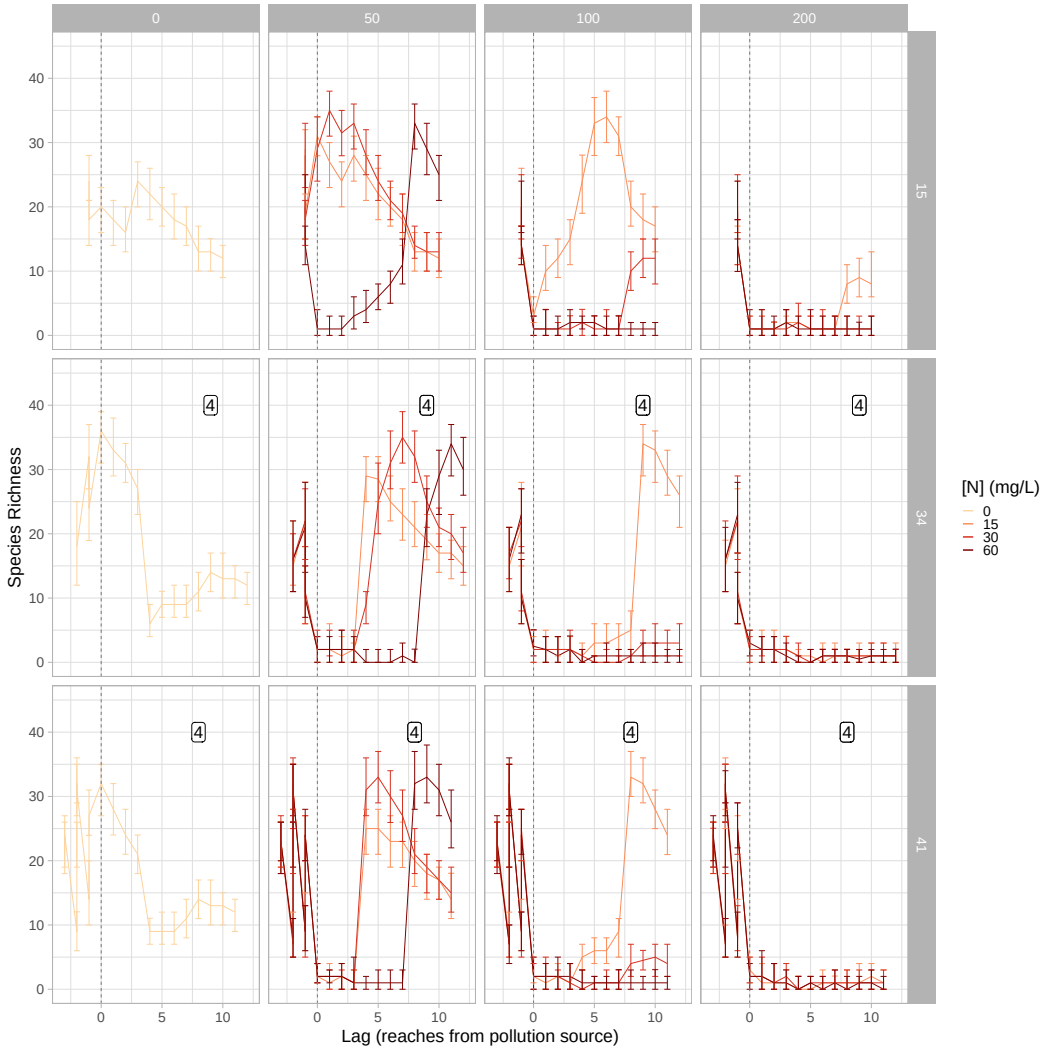

Figure 6: Comparison of asv richness across all scenarios. Lag values indicate the number of reaches downstream of the pollution source (which is marked with a dashed line). Columns indicate the discharge of the pollution source, ranging from 0 (control) to 200 L/s. Rows indicate the reach where pollution was applied. Error bars show 95% quantile ranges across repeated simulations. In some scenarios, reach 4 became a diversity hotspot, and is indicated with a text label.

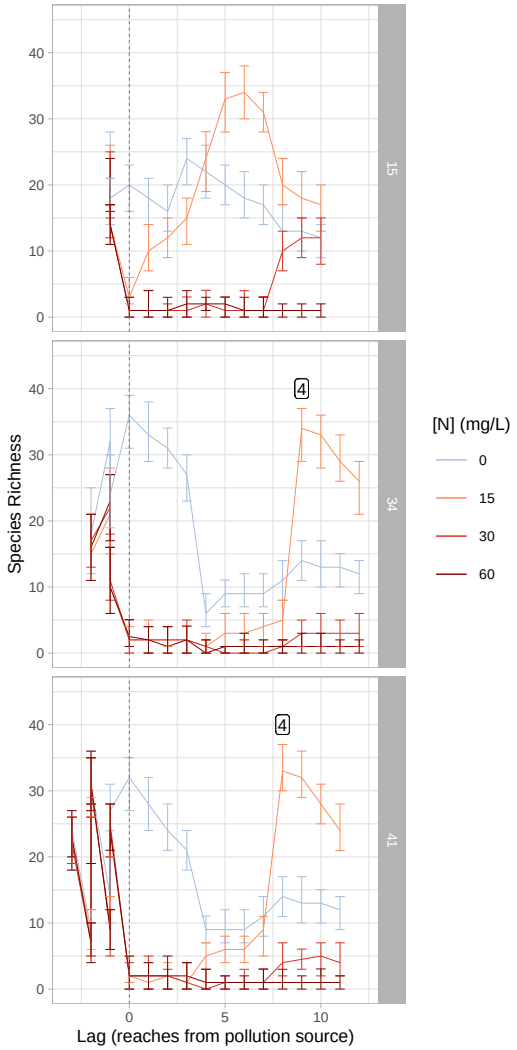

Figure 7: Comparison of asv richness across all scenarios. Lag values indicate the number of reaches downstream of the pollution source (which is marked with a dashed line). Pollution discharge was 100 L/s. Row labels indicate the reach where pollution was applied. Error bars show 95% quantile ranges across repeated experiments. In some scenarios, reach 4 became a diversity hotspot, and is indicated with a text label.

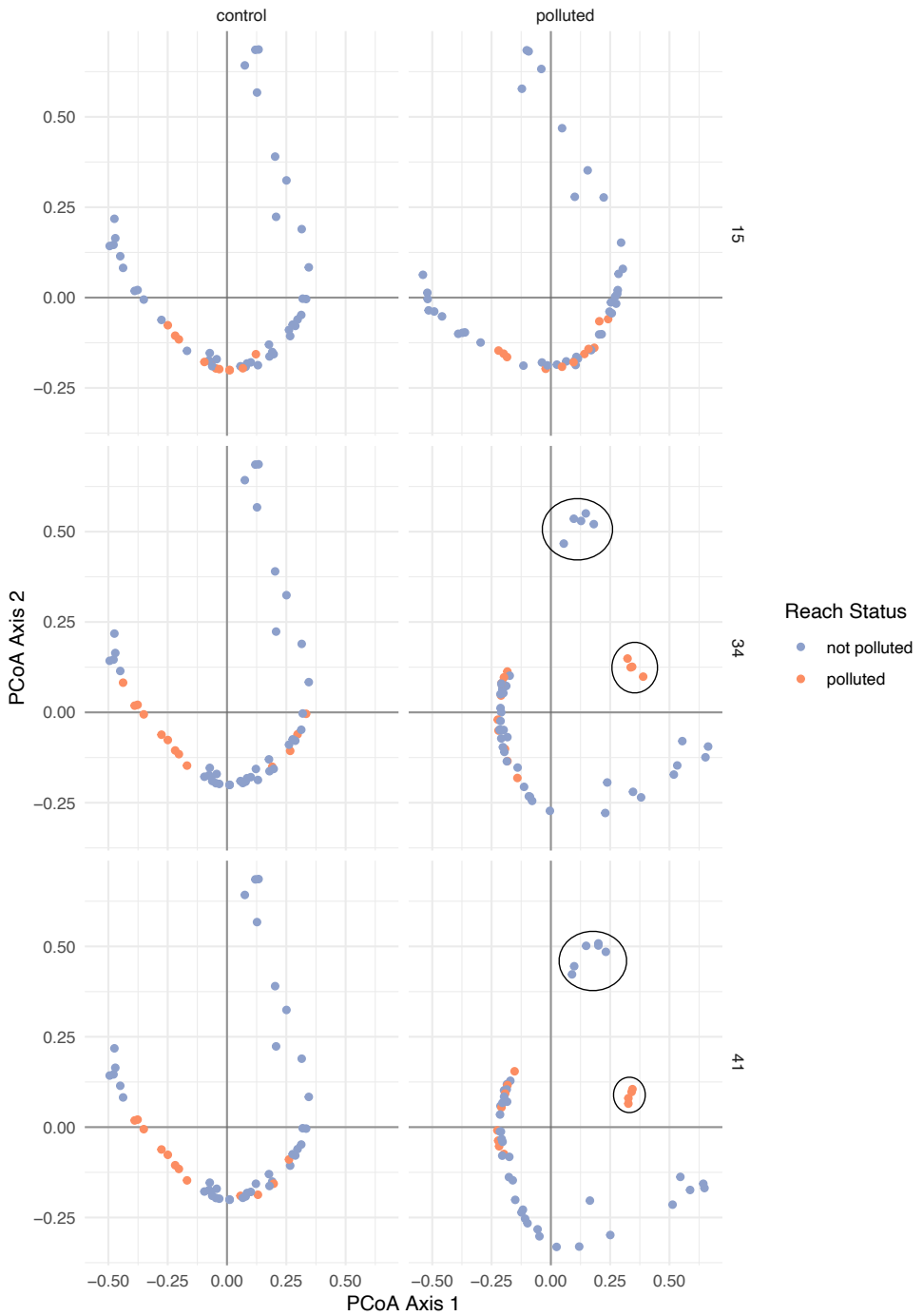

Figure 8: Comparison of community composition between control (left) and pollution (right) treatments for three different pollution origins (rows). In all cases, the weakest pollution treatment (i.e., 15 mg/L at 50 L/s) was used. There was little impact on community composition when reach 15 was polluted. For the other two origins, both polluted and non-polluted reaches developed unique communities (circled) relative to the control.

4 Discussion

We have presented a new model for interacting community and resource dynamics in fluvial meta-ecosystems, along with an R-package *flume* implementing the model (Talluto 2023). Our model is based on coupling a patch dynamics model (similar to classical metapopulation models; Levins 1969) with a reaction transport model. We demonstrate with our case studies that the model can be used to explore hypotheses about the mechanisms structuring biodiversity-EF relationships and metacommunity structure. In the first case study, the model reproduced a theoretically predicted hump-shaped relationship between dispersal and the biodiversity-EF slope under specific conditions. In particular, the hump shape was only visible when competition was a strong influence in structuring the biological community, and was more pronounced with more diverse metacommunities (Fig. 4). Variation in the output across replicate simulations and due to different species in the metacommunities was low relative to the magnitude of the effects. In the second case study, we partially parameterised the model with data from a field study, then manipulated nutrient inputs to simulate point-source pollution. High levels of pollution had strong effects on both richness and community composition, with effects that reached far beyond the local reach receiving nitrogen input (Figs. 5, 7, 8). Some partially affected reaches became diversity hotspots, and even non-polluted reaches experienced changes in community composition (Fig. 8).

Movements of resources and organisms in meta-ecosystems can have profound implications for ecosystem structure and function (Sabo and Hagen 2012). Nutrient fluxes in particular can mediate diversity and stability in local communities, and can impact the trait distribution within local communities (Gravel et al. 2010). The extent to which ecosystems exchange resources and the degree to which this exchange imposes costs and benefits on each ecosystem can lead to complex dynamics, including alternative stable states (Messan et al. 2018). In rivers, cross-ecosystem fluxes of both organisms and material are facilitated by the flow of water, and are a dominant feature structuring both biological communities and habitats. Thus, meta-ecosystem models in rivers must account for these very high cross-ecosystem flows while also accounting for interactions both within local biological communities and between communities and resources. Moreover, the match of organisms to resource conditions can strongly influence EF (Talluto et al. 2024). Our first case study demonstrates this point, with stronger relationships between biodiversity and EF when high gamma diversity and high dispersal rates facilitate organisms reaching habitats where their fitness is highest (Fig. 4).

4.1 Applications

One of the main applications of our model and the accompanying software is in rapidly exploring hypotheses relating to diversity and EF at the scale of entire river networks. Conducting field or laboratory experiments at the scale of entire networks can be cost-prohibitive, whereas manifold manipulations can easily be performed *in silico* (Tonkin et al. 2018). For example, changes in river network topology (e.g., due to human influence or changing precipitation patterns) can influence the balance between resource consumption and transport, and also change metacommunity dynamics (and associated feedbacks between the community and resource con-

sumption). In the field, such changes can be studied either in time (e.g., by studying a single network before and after disruption), or in space (e.g., studying many networks with different spatial properties), but in both cases such studies are expensive and logistically difficult. Our model could be used to explore potentially fruitful avenues of research, to suggest experimental designs, and to evaluate potential mechanisms before committing resources to a field study.

Large-scale flow experiments, often in association with changes in managed flow regimes downstream of large dams, are one way to test connectivity changes across a significant portion of a river network (Konrad et al. 2011). However, these experiments are expensive and necessarily involve multiple stakeholders with potentially competing interests, and not all such experiments will have the resources to collect the relevant ecological data at meta-ecosystem scales (Olden et al. 2014; Kuemmerlen et al. 2019). Moreover, many experimental manipulations that might be physically feasible (e.g., pollution, changes in land use, invasive species) cannot be performed for ethical reasons due to their environmental impact. Experiments of this sort must be done in the laboratory, where spatial scale is often limiting and scaling rules are poorly understood, or opportunistically, when natural or anthropogenic events produce the desired manipulations. Indeed, when such manipulations are planned (e.g., dam construction or removal), our model can be used to experiment in advance with potential scenarios, informing field data collection or providing information about the range of possible impacts and restoration outcomes.

4.2 Calibration

Calibration of our model presents a number of challenges. Although the model parameters describe ecological processes, many of them will be very difficult to measure in practice. For example, measuring dispersal rates is possible, but our model expects dispersal in terms of the contribution to total colonisation flux (and incorporates both the movement of organisms as well as the successful establishment at the colonisation site). This is nearly impossible to measure in the field, although it could be measured or controlled for in laboratory conditions. However, measurement of dispersal in terms of relative rates of upstream and downstream dispersal is possible, as is estimation of dispersal kernels; this could still be useful for calibration by establishing relationships among model parameters.

At a higher level, many of the model's outputs are frequently measured under field conditions, such as bulk rates of EF or local and regional biodiversity patterns. Thus, inverse calibration becomes possible. Such a procedure would involve obtaining information from field or lab experiments that correspond to particular model outputs (as well as inputs when possible). Then the calibration algorithm searches for parameter combinations that maximise the likelihood of the measured quantities given the model outputs. Because the model has many free parameters, some of which are likely exchangeable, simple optimisation algorithms are unlikely to produce sensible results. However, algorithms that perform better with multiple local optima, such as simulated annealing or Markov Chain Monte Carlo (MCMC) may be fruitful. Bayesian calibration using MCMC in particular has two benefits. First, a modeller can constrain model parameters using prior distributions, helping to narrow the search space and making it less likely that the model produces unrealistic parameter estimates. Second, full posterior inference allows for multiple parameter combinations to be included in the solution set and compared

probabilistically. For example, a given data set may reveal that either active dispersal and competition are both very high, or dispersal and competition are very low, but only if there is also immigration from outside the river network. This kind of exercise could prove very useful in suggesting hypotheses and guiding future field studies. A major challenge of this approach is computational; MCMC may require many model runs to fully explore the parameter space, especially for high-dimensional models.

References

Altermatt, Florian, Chelsea J. Little, Elvira Mächler, Shaopeng Wang, Xiaowei Zhang et al. (2020). Uncovering the Complete Biodiversity Structure in Spatial Networks: The Example of Riverine Systems. *Oikos* 129.5, pp. 607–618.

Austin, Mike P. (1999). A Silent Clash of Paradigms: Some Inconsistencies in Community Ecology. *Oikos* 86.1, pp. 170–178.

Baird, Donald J. and Mehrdad Hajibabaei (2012). Biomonitoring 2.0: A New Paradigm in Ecosystem Assessment Made Possible by next-Generation DNA Sequencing. *Molecular Ecology* 21.8, pp. 2039–2044.

Bannar-Martin, Katherine H., Colin T. Kremer, S.K. Morgan Ernest, Mathew A. Leibold, Harald Auge et al. (2018). Integrating Community Assembly and Biodiversity to Better Understand Ecosystem Function: The Community Assembly and the Functioning of Ecosystems (CAFE) Approach. *Ecology Letters* 21.2, pp. 167–180.

Battin, Tom J., Louis A. Kaplan, Stuart Findlay, Charles S. Hopkinson, Eugenia Marti et al. (Feb. 2008). Biophysical Controls on Organic Carbon Fluxes in Fluvial Networks. *Nature Geoscience* 1.2, pp. 95–100.

Burgers, H. E. (Robin), Aafke M. Schipper and A. Jan Hendriks (2014). Size Relationships of Water Discharge in Rivers: Scaling of Discharge with Catchment Area, Main-Stem Length and Precipitation. *Hydrological Processes* 28.23, pp. 5769–5775.

Callahan, Benjamin J, Paul J McMurdie and Susan P Holmes (1st Dec. 2017). Exact Sequence Variants Should Replace Operational Taxonomic Units in Marker-Gene Data Analysis. *The ISME Journal* 11.12, pp. 2639–2643.

Callahan, Benjamin J., Paul J. McMurdie, Michael J. Rosen, Andrew W. Han, Amy Jo A. Johnson et al. (July 2016). DADA2: High-resolution Sample Inference from Illumina Amplicon Data. *Nature Methods* 13.7, pp. 581–583.

Cardinale, Bradley J., J. Emmett Duffy, Andrew Gonzalez, David U. Hooper, Charles Perrings et al. (7th June 2012). Biodiversity Loss and Its Impact on Humanity. *Nature* 486.7401, pp. 59–67.

Cid, Núria, Tibor Erős, Jani Heino, Gabriel Singer, Sonja C Jähnig et al. (2022). From Meta-System Theory to the Sustainable Management of Rivers in the Anthropocene. *Frontiers in Ecology and the Environment* 20.1, pp. 49–57.

Cornwell, William K., Johannes H. C. Cornelissen, Kathryn Amatangelo, Ellen Dorrepaal, Valerie T. Eviner et al. (2008). Plant Species Traits Are the Predominant Control on Litter Decomposition Rates within Biomes Worldwide. *Ecology Letters* 11.10, pp. 1065–1071.

Declerck, Steven A. J., Christian Winter, Jonathan B. Shurin, Curtis A. Suttle and Blake Matthews (Mar. 2013). Effects of Patch Connectivity and Heterogeneity on Metacommunity Structure of Planktonic Bacteria and Viruses. *The ISME Journal* 7.3 (3), pp. 533–542.

Díaz, Sandra, Andy Purvis, Johannes H. C. Cornelissen, Georgina M. Mace, Michael J. Donoghue et al. (2013). Functional Traits, the Phylogeny of Function, and Ecosystem Service Vulnerability. *Ecology and Evolution* 3.9, pp. 2958–2975.

Díaz, Sandra, Amy J. Symstad, F. Stuart Chapin, David A. Wardle and Laura F. Huenneke (1st Mar. 2003). Functional Diversity Revealed by Removal Experiments. *Trends in Ecology & Evolution* 18.3, pp. 140–146.

Directive 91/271/EEC (1991). Council Directive 91/271/EEC of 21 May 1991 Concerning Urban Waste Water Treatment. *Official Journal of the European Communities L* 135 (30.5.1991), pp. 40–52.

Duffy, J. Emmett, Casey M. Godwin and Bradley J. Cardinale (Sept. 2017). Biodiversity Effects in the Wild Are Common and as Strong as Key Drivers of Productivity. *Nature* 549.7671, pp. 261–264.

Fernández-Nava, Y., E. Marañón, J. Soons and L. Castrillón (1st Nov. 2008). Denitrification of Wastewater Containing High Nitrate and Calcium Concentrations. *Bioresource Technology* 99.17, pp. 7976–7981.

Fuß, Thomas, Lukas Thuile Bistarelli, Robert Ptacnik and Gabriel Singer (2024a). Niche Partitioning in a Periphyton Metacommunity Peaks at Intermediate Species Richness in Mid-Sized Rivers. *Ecology* in press.

Fuß, Thomas, Lukas Thuile Bistarelli, Franziska Walther, Simon Vitecek, Lauren Talluto et al. (12th June 2024b). Geodiversity of a European River Network Controls Algal Biodiversity and Function. *Communications Earth & Environment* 5.1, pp. 1–13.

Gagic, Vesna, Ignasi Bartomeus, Tomas Jonsson, Astrid Taylor, Camilla Winqvist et al. (22nd Feb. 2015). Functional Identity and Diversity of Animals Predict Ecosystem Functioning Better than Species-Based Indices. *Proceedings of the Royal Society B: Biological Sciences* 282.1801, p. 20142620.

Gounand, Isabelle, Eric Harvey, Chelsea J. Little and Florian Altermatt (1st Jan. 2018). Meta-Ecosystems 2.0: Rooting the Theory into the Field. *Trends in Ecology & Evolution* 33.1, pp. 36–46.

Gravel, Dominique, Nicolas Mouquet, Michel Loreau and Frédéric Guichard (Sept. 2010). Patch Dynamics, Persistence, and Species Coexistence in Metaecosystems. *The American Naturalist* 176.3, pp. 289–302.

Harvey, Eric, Justin N. Marleau, Isabelle Gounand, Shawn J. Leroux, Carina R. Firkowski et al. (2023). A General Meta-Ecosystem Model to Predict Ecosystem Functions at Landscape Extents. *Ecography* 2023.11, e06790.

Heino, Jani, Adriano S. Melo, Tadeu Siqueira, Janne Soininen, Sebastian Valanko et al. (2015). Metacommunity Organisation, Spatial Extent and Dispersal in Aquatic Systems: Patterns, Processes and Prospects. *Freshwater Biology* 60.5, pp. 845–869.

Holt, R. D., J. H. Lawton, K. J. Gaston and T. M. Blackburn (1997). On the Relationship between Range Size and Local Abundance: Back to Basics. *Oikos* 78.1, pp. 183–190.

Holt, R.d. and T.h. Keitt (2000). Alternative Causes for Range Limits: A Metapopulation Perspective. *Ecology Letters* 3.1, pp. 41–47.

Holt, Robert D., Timothy H. Keitt, Mark A. Lewis, Brian A. Maurer and Mark L. Taper (2005). Theoretical Models of Species' Borders: Single Species Approaches. *Oikos* 108.1, pp. 18–27.

Hooper, D. U., F. S. Chapin III, J. J. Ewel, A. Hector, P. Inchausti et al. (2005). Effects of Biodiversity on Ecosystem Functioning: A Consensus of Current Knowledge. *Ecological Monographs* 75.1, pp. 3–35.

Hooper, David U., E. Carol Adair, Bradley J. Cardinale, Jarrett E. K. Byrnes, Bruce A. Hungate et al. (June 2012). A Global Synthesis Reveals Biodiversity Loss as a Major Driver of Ecosystem Change. *Nature* 486.7401 (7401), pp. 105–108.

Horváth, Zsófia, Csaba F. Vad and Robert Ptacnik (2016). Wind Dispersal Results in a Gradient of Dispersal Limitation and Environmental Match among Discrete Aquatic Habitats. *Ecography* 39.8, pp. 726–732.

Huber Stefan A. amd Balz, A, M. Abert and W Pronk (2011). Characterisation of Aquatic Humic and Non-Humic Matter with Size-Exclusion Chromatography – Organic Carbon Detection – Organic Nitrogen Detection (LCOCD-OND). *Water Research* 45.5, pp. 879–885.

Hunt, Julia J.F.G. and Michael B. Bonsall (2009). The Effects of Colonization, Extinction and Competition on Co-Existence in Metacommunities. *Journal of Animal Ecology* 78.4, pp. 866–879.

Konrad, Christopher P., Julian D. Olden, David A. Lytle, Theodore S. Melis, John C. Schmidt et al. (1st Dec. 2011). Large-Scale Flow Experiments for Managing River Systems. *BioScience* 61.12, pp. 948–959.

Kristiansen, Jørgen (1st Oct. 1996). 16. Dispersal of Freshwater Algae — a Review. *Hydrobiologia* 336.1, pp. 151–157.

Kuemmerlen, Mathias, Peter Reichert, Rosi Siber and Nele Schuwirth (10th Feb. 2019). Ecological Assessment of River Networks: From Reach to Catchment Scale. *Science of The Total Environment* 650, pp. 1613–1627.

Leibold, M. A., M. Holyoak, N. Mouquet, P. Amarasekare, J. M. Chase et al. (2004). The Metacommunity Concept: A Framework for Multi-Scale Community Ecology. *Ecology Letters* 7.7, pp. 601–613.

Levins, Richard (1st Sept. 1969). Some Demographic and Genetic Consequences of Environmental Heterogeneity for Biological Control1. *Bulletin of the Entomological Society of America* 15.3, pp. 237–240.

Little, Chelsea J. and Florian Altermatt (2018). Species Turnover and Invasion of Dominant Freshwater Invertebrates Alter Biodiversity–Ecosystem-Function Relationship. *Ecological Monographs* 88.3, pp. 461–480.

Loreau, Michel, Nicolas Mouquet and Robert D. Holt (2003). Meta-Ecosystems: A Theoretical Framework for a Spatial Ecosystem Ecology. *Ecology Letters* 6.8, pp. 673–679.

Margalef, R. (Nov. 1963). On Certain Unifying Principles in Ecology. *The American Naturalist* 97.897, pp. 357–374.

McGill, Brian J. (1st Mar. 2012). Trees Are Rarely Most Abundant Where They Grow Best. *Journal of Plant Ecology* 5.1, pp. 46–51.

Messan, Marisabel Rodriguez, Darin Kopp, Daniel C. Allen and Yun Kang (1st July 2018). Dynamical Implications of Bi-Directional Resource Exchange within a Meta-Ecosystem. *Mathematical Biosciences* 301, pp. 167–184.

Mouquet, Nicolas and Michel Loreau (Nov. 2003). Community Patterns in Source-Sink Metacommunities. *The American Naturalist* 162.5, pp. 544–557.

Olden, Julian D, Christopher P Konrad, Theodore S Melis, Mark J Kennard, Mary C Freeman et al. (2014). Are Large-Scale Flow Experiments Informing the Science and Management of Freshwater Ecosystems? *Frontiers in Ecology and the Environment* 12.3, pp. 176–185.

Pennekamp, Frank, Mikael Pontarp, Andrea Tabi, Florian Altermatt, Roman Alther et al. (Nov. 2018). Biodiversity Increases and Decreases Ecosystem Stability. *Nature* 563.7729 (7729), pp. 109–112.

Roebuck, Jesse Alan Jr., Michael Seidel, Thorsten Dittmar and Rudolf Jaffé (7th Jan. 2020). Controls of Land Use and the River Continuum Concept on Dissolved Organic Matter Composition in an Anthropogenically Disturbed Subtropical Watershed. *Environmental Science & Technology* 54.1, pp. 195–206.

Sabo, John L. and Elizabeth M. Hagen (2012). A Network Theory for Resource Exchange between Rivers and Their Watersheds. *Water Resources Research* 48.4.

Sleighter, Rachel L. and Patrick G. Hatcher (June 2008). Molecular Characterization of Dissolved Organic Matter (DOM) along a River to Ocean Transect of the Lower Chesapeake Bay by Ultrahigh Resolution Electrospray Ionization Fourier Transform Ion Cyclotron Resonance Mass Spectrometry. *Marine Chemistry* 110.3-4, pp. 140–152.

Soetaert, Karline and Peter MJ Herman (2009). *A Practical Guide to Ecological Modelling.* Berlin: Springer.

Soetaert, Karline, Thomas Petzoldt and R. Woodrow Setzer (23rd Feb. 2010). Solving Differential Equations in R: Package deSolve. *Journal of Statistical Software* 33, pp. 1–25.

Stelzer, Robert S. and Gary A. Lamberti (2001). Effects of N: P Ratio and Total Nutrient Concentration on Stream Periphyton Community Structure, Biomass, and Elemental Composition. *Limnology and Oceanography* 46.2, pp. 356–367.

Talluto, Lauren (2023). *Flume: A Model For Fluvial Meta-Ecosystems. https://github.com/flee-group/flume.* Version 0.5.1.9002.

Talluto, Lauren, Isabelle Boulangeat, Steve Vissault, Wilfried Thuiller and Dominique Gravel (12th June 2017). Extinction Debt and Colonization Credit Delay Range Shifts of Eastern North American Trees. *Nature Ecology & Evolution* 1.7 (7), pp. 1–6.

Talluto, Lauren, Rubén del Campo, Edurne Estévez, Florian Altermatt, Thibault Datry et al. (2024). Towards (better) fluvial meta-ecosystem ecology: a research perspective. *npj Biodiversity* 3.3.

Thébault, Elisa and Michel Loreau (1st Jan. 2006). The Relationship between Biodiversity and Ecosystem Functioning in Food Webs. *Ecological Research* 21.1, pp. 17–25.

Tonkin, Jonathan D., Florian Altermatt, Debra S. Finn, Jani Heino, Julian D. Olden et al. (2018). The Role of Dispersal in River Network Metacommunities: Patterns, Processes, and Pathways. *Freshwater Biology* 63.1, pp. 141–163.

Tremblay, Luc, Ghita Alaoui and Marc N. Léger (15th Nov. 2011). Characterization of Aquatic Particles by Direct FTIR Analysis of Filters and Quantification of Elemental and Molecular Compositions. *Environmental Science & Technology* 45.22, pp. 9671–9679.

Urban, Mark C. (2004). Disturbance Heterogeneity Determines Freshwater Metacommunity Structure. *Ecology* 85.11, pp. 2971–2978.

Visco, Joana Amorim, Laure Apothéloz-Perret-Gentil, Arielle Cordonier, Philippe Esling, Loïc Pillet et al. (7th July 2015). Environmental Monitoring: Inferring the Diatom Index from Next-Generation Sequencing Data. *Environmental Science & Technology* 49.13, pp. 7597–7605.

Winfree, Rachael, Jeremy W. Fox, Neal M. Williams, James R. Reilly and Daniel P. Cariveau (2015). Abundance of Common Species, Not Species Richness, Drives Delivery of a Real-World Ecosystem Service. *Ecology Letters* 18.7, pp. 626–635.

Zimmermann, Jonas, Gernot Glöckner, Regine Jahn, Neela Enke and Birgit Gemeinholzer (2015). Metabarcoding vs. Morphological Identification to Assess Diatom Diversity in Environmental Studies. *Molecular Ecology Resources* 15.3, pp. 526–542.

Zimmermann, Jonas, Regine Jahn and Birgit Gemeinholzer (1st July 2011). Barcoding Diatoms: Evaluation of the V4 Subregion on the 18S rRNA Gene, Including New Primers and Protocols. *Organisms Diversity & Evolution* 11.3, pp. 173–192.